Frontiers of Physics
https://doi.org/10.1007/s11467-020-0997-x
Front. Phys.
16(1), 13305 (2021)

TOPICAL REVIEW

Nonideal double-slope effect in organic field-effect transistors

Ming-Chao Xiao[1,2], Jie Liu[2], Yuan-Yuan Hu[3,†], Shuai Wang[1,‡], Lang Jiang[2,#]

[1] *Key Laboratory of Material Chemistry for Energy Conversion and Storage, Ministry of Education, School of Chemistry and Chemical Engineering, Huazhong University of Science and Technology, Wuhan 430074, China*
[2] *Beijing National Laboratory for Molecular Sciences, Institute of Chemistry Chinese Academy of Sciences, Beijing 100190, China*
[3] *Key Laboratory for Micro-Nano Optoelectronic Devices of Ministry of Education, School of Physics and Electronics, Hunan University, Changsha 410082, China*
Corresponding authors. E-mail: [†] *yhu@hnu.edu.cn,* [‡] *chmsamuel@mail.hust.edu.cn,* [#] *ljiang@iccas.ac.cn*
Received July 20, 2020; accepted August 22, 2020

With the development of device engineering and molecular design, organic field effect transistors (OFETs) with high mobility over 10 $cm^2 \cdot V^{-1} \cdot s^{-1}$ have been reported. However, the nonideal double-slope effect has been frequently observed in some of these OFETs, which makes it difficult to extract the intrinsic mobility OFETs accurately, impeding the further application of them. In this review, the origin of the nonideal double-slope effect has been discussed thoroughly, with affecting factors such as contact resistance, charge trapping, disorder effects and coulombic interactions considered. According to these discussions and the understanding of the mechanism behind double-slope effect, several strategies have been proposed to realize ideal OFETs, such as doping, molecular engineering, charge trapping reduction, and contact engineering. After that, some novel devices based on the nonideal double-slope behaviors have been also introduced.

Keywords organic field effect transistors, nonideal double-slope effect, mobility

Contents

1 Introduction 1
2 Mechanisms of nonideal double-slope OFETs 2
2.1 Contact resistance effects 2
2.2 Charge trapping effects 3
2.3 Disorder effects and Coulombic interactions 3
3 Strategies for reducing the nonideal behaviors 4
3.1 Doping and molecular engineering 4
3.2 Reducing charge trapping 8
3.3 Contact engineering 8
4 Utilizations of nonideal OFETs 9
5 Conclusions and outlook 10
Acknowledgements 10
References 11

1 Introduction

Organic electronics has attracted extensive attention for their unique properties, such as light-weight, flexibility, low-cost solution-processability, and molecularly designable ability for special photoelectric performance [1–18]. A mass of applications based on organic electronics have been developed such as organic photovoltaics (OPVs), organic light-emitting diodes (OLEDs), organic field-effect transistors (OFETs), and organic memories [2, 19–24]. Among them, OFET is one of the fundamental elements for organic electronics, and a powerful tool to develop high performance organic circuits, sensors and other applications [25–27].

The parameters used to describe electrical properties of OFETs are commonly calculated by using the classical metal oxide-semiconductor field-effect transistor (MOSFET) model [28, 29]. Mobility is a key parameter to describe electrical properties of OFETs. With the development of molecular design and device engineering, a mass of high mobility organic materials have been reported, in which the mobility of *p*-type organic semiconductors is over 20 $cm^2 \cdot V^{-1} \cdot s^{-1}$ and that of *n*-type ones is over 10 $cm^2 \cdot V^{-1} \cdot s^{-1}$ [30–40]. Despite the remarkable mobility values of OFETs, many of them exhibit nonideal behaviors such as double-slope effect, which means the drain current I_d as a function of gate voltage V_g (or square root of drain current $I_d^{1/2}$) shows an abrupt change in the slope in the linear regime (or saturation regime) [see Figs. 1(a) and (b)] [38, 42, 46]. The nonideal double-slope effect has brought difficulties to the calcu-

*Special Topic: Organic Semiconductors and OFETs (Eds. Hong Meng & Guangcun Shan). This article can also be found at http://journal.hep.com.cn/fop/EN/10.1007/s11467-020-0997-x.

© Higher Education Press 2021

lation of OFET's parameters and the commercial applications of OFETs such as OFET-driven flexible OLED displays [29, 33, 36, 41–46]. To understand the nonideal double-slope effect, several possible mechanisms have been proposed, such as the abrupt change in contact resistance, the charge trapping at the semiconductor/dielectric interface, the different disorder degrees in the bulk of semiconductors, coulombic interaction between charge carriers and charge injection from the conducting channel into the dielectric layer [6, 29, 33, 46–48]. Overall, by far we have not arrived consensus on understanding the physics behind the nonideal double-slope effect.

In this review, we first introduce the different mechanisms proposed for explaining the nonideal double-slope effect. Then we have summarized some strategies to reduce or mitigate the nonideal behaviors in OFETs. After that, the utilization of nonideal double-slope OFETs are discussed. Finally, the conclusions and perspectives are given about the study of the nonideal double-slope effect.

2 Mechanisms of nonideal double-slope OFETs

2.1 Contact resistance effects

Contact resistance at the interface between electrodes and semiconductors has a profound effect on the effective mobility [49–52]. In OFETs, contact resistance not only affects the performance of devices, but also contribute to the occurring of nonideal double-slope effect. Some literatures have investigated and analyzed the influence of contact resistance on nonideal behaviors theoretically and experimentally [29, 53–59].

It is well known that contact resistance in OFETs is not a constant value, but one decreasing gradually with increasing gate bias [29, 46, 60, 61]. Gundlach *et al.* proposed that the mobility is overestimated from OFETs with double-slope effect, and they argued this effect arises from the gate-bias dependence of the contact resistance [29], as shown in Figs. 1(c)–(f). The most commonly used model to calculate mobility is the MOSFET model. In an ideal OFET, the I_d (or $I_d{}^{1/2}$) as a function of V_g exhibits a single constant slope in the linear regime (or saturation regime). As for nonideal OFETs, two slopes under different gate bias are obtained. The mobility obtained from the two different slopes can be more than 6–7 times different [Figs. 1(c) and (d)]. By using the impedance spectroscopy, they extracted the gate dependence of contact resistance [Fig. 1(e)]. It was seen that in the low V_g regime, the contact resistance decreases with V_g much more significantly than the channel resistance. They demonstrated that this stronger gate dependence of contact resistance could induce the double-slope behaviors by simulations [Fig. 1(f)].

In accordance with the above discussions, Liu *et al.* proposed that the nonideal behaviors of transfer characteristics come from the evolution of the injection barrier and band bending (Fig. 2) [57]. In the linear regime, the behaviors are directly related to the varying of contact resistance. When the contact resistance is larger than channel resistance and decreases rapidly, the voltage drop on the channel increases with the gate bias, which results in the overestimation of mobility, as shown in Figs. 2(a)–(c). It means that the nonideal double-slope effect come from the varying of the contact resistance in linear regime. However, we usually extract the mobility from the transfer curves in saturation regime. As for the saturation regime, the mechanism becomes more complicated [Figs. 2(d)–(g)]. The band bending affects the injection and the potential distribution in the OFETs. At low gate bias ($|V_g| < 30$ V), the devices work with Schottky contacts. The carriers pass the depletion region by thermal emission, which causes high resistance. Thus, most of the voltage is distributed on the contact area [Fig. 2(f)], inducing the much lower channel current or mobility. At high gate bias ($|V_g| > 40$ V), the carriers mainly tunnel across the barrier with strong bending of the valence band and the narrowing of the barrier width [Fig. 2(g)], which induces the Ohmic-like contacts [$V_g = -70$ V, Fig. 2(e)]. This tran-

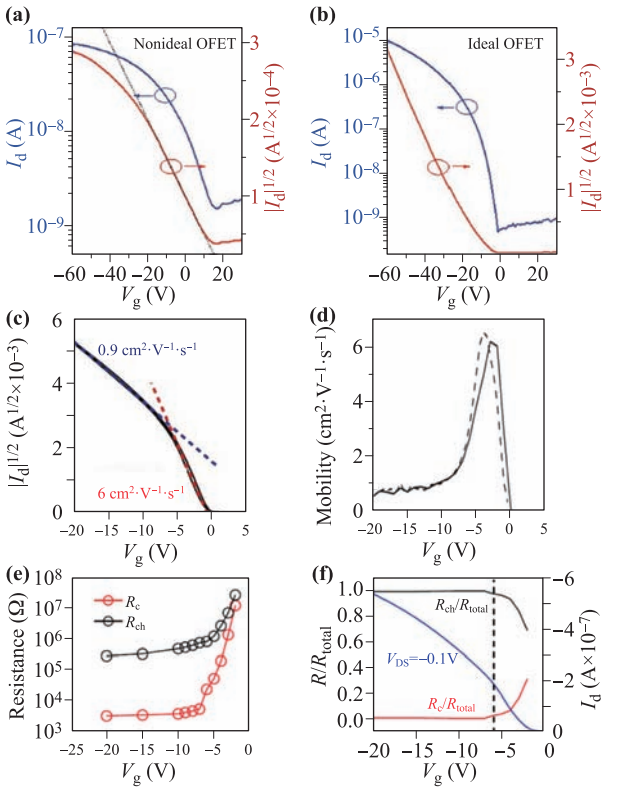


Fig. 1 **(a, b)** Transfer characteristics of nonideal OFET (a) and ideal OFET (b). Reproduced from Ref. [6]. **(c)** Transfer curves of rubrene OFET with double-slope characteristics; **(d)** Mobility extracted from MOSFET model under different gate bias; **(e)** Contact resistance (R_c) and channel resistance (R_{ch}) under gate bias; **(f)** Plot of the I–V characteristic along with plot of R_c/R_{total} and R_{ch}/R_{total}(R_{total} for total resistance). Reproduced from Ref. [29].

sition from Schottky contact transistor working mode to normal MOSFET mode leads to the double-slope behaviors, as illustrated in Fig. 2(d). In addition to the device simulation results, the same group have carried out experimental work to verify this idea by developing a general approach to probe the carrier mobility in OFETs with nonuniform charge accumulation [62, 63].

In general, contact resistance acts as the important role in the nonideal double-slope effect. The varying contact resistance in linear regime and the band bending, charge injection in saturation regime can be the reason of the nonideal behaviors. Therefore, achieving Ohmic source/drain contacts through contact engineering is critical for removing the non-ideal behaviors in OFETs.

2.2 Charge trapping effects

In addition to contact resistance effects, some literatures reported that charge trapping effects induce the nonideal double-slope behaviors [6, 48]. As well known, in an *n*-type OFETs, the silanol group (–SiOH) on the SiO_2 substrate causes electron trapping and the formation of the $–SiO^-$ [48]. It also has been proved that the production of $–SiO^-$ comes from the electrochemical reactions of water, oxygen, silanol and trapped electrons [64–67].

Recently, it is noticed that polymer field effect transistors more likely exhibit the nonideal double-slope characteristics, especially for donor-acceptor (D–A) polymers [36, 37, 43, 45, 68, 69]. Nguyen *et al.* found some interesting phenomena [48], namely the PCDTPT (a donor-acceptor copolymer) OFETs exhibit ideal transfer characteristic behaviors and show strong ambipolarity in the first scan of transfer curves. However, the double-slope phenomenon occurs after the devices were in operation for 5 mins [Figs. 3(a) and (b)]. As the device was bias-stressed in the electron conduction regime ($V_g = +30$ V), a significant change in the transfer curve was observed in electron conduction regime, as shown in Fig. 3(c). The current decay as a function of bias-stress time also shows that the drain current decreased seriously in electron conduction regime [Fig. 3(d)]. After studying the evolving of transfer characteristics of PCDTPT OFETs under bias-stress, they proved that electron trapping at the gate dielectric/semiconductor interface greatly alters the device characteristics and accounts for the occurrence of the double slope. They also proposed that a trace amount of water trapped in devices contributes to the nonideal double-slope effect, as shown in Figs. 3(e) and (f). The current decay of bias-stress time is effectively suppressed in the device with BCB (a water repelled polymer) as dielectrics.

However, this mechanism cannot apply to the nonideal behaviors observed in single crystal OFETs or unipolar OFETs, because in these devices, the trapping of minority charge carriers is difficult to happen. To cope with this inconsistency, Pei *et al.* proposed a new mechanism to explain the double slope effect involving charge trapping, which is independent with the conductor layer and the carrier types (Fig. 4) [6]. They directly observed the charge trapping process by using scanning Kelvin probe microscopy (SKPM), as shown in Figs. 4(a)–(d). At $V_g = 10$ V, the charge trapping progress occurs on the surface of the dielectric and evolves with time. After the gate bias was switched to $V_g = 0$ V, the accumulated charges were neutralized or detrapped gradually. By employing dielectrics with different functional groups, they found that the nonideal double-slope behaviors come from the electrochemical reactions happened on/in the dielectric layers. Then, they explored the impact of gate bias, –SiOH, water and oxygen in charge trapping progress [Figs. 4(e)–(h)]. Similar to the $–SiO^-$ on the SiO_2, they also found that the –OH, $–NH_2$, and –COOH which are commonly seen in organic dielectrics can also induce charge trapping. They proposed that gate bias, active functional groups, and adsorbed water plays the important roles in the trapping process, inducing the nonideal double-slope behaviors.

To summarize, the charge trapping process happened in the dielectrics is caused by the electrochemical reactions between the functional groups, gate bias and a trace amount of water trapped in the semiconductors, which induce the nonideal double-slope behaviors. These literatures provide new insights for understanding the nonideal double-slope effects. Moreover, they point out that reducing charge trapping effects could be an effective strategy for achieving ideal OFETs.

2.3 Disorder effects and Coulombic interactions

In addition to the effects of charge trapping and contact resistance on nonideal double-slope behaviors, some other possible mechanisms have been proposed, such as disorder effects and coulombic interactions [33, 47]. Similar to the polymer FETs, the nonideal double-slope phenomenon have been observed in small molecule crystal FETs, such as rubrene single-crystal devices [33]. In such cases, Takeya *et al.* argued that the nonideal double-slope phenomenon was attributed to the disorder of crystals. They proposed that at low gate bias, the electric field can penetrate into the crystal and the accumulation layer forms in the inner crystal. Thus, the charge carriers are less affected by the random potentials of dielectrics, and a higher mobility is obtained. When the device works at high gate bias, the carriers are tightly bound at the interface and is affected by the scattering of the interface, which induces the lower mobility. Morpurgo *et al.* also observed the nonideal double-slope behaviors in rubrene crystals FETs [47]. They proposed that higher density of carriers under high gate bias makes the carriers very crowded where the average distance between the carriers is only a few molecules in size. In this case, the long-range coulombic interactions between carriers are negligible and they can induce the increase of the hopping activation barrier, causing the nonideal behaviors.

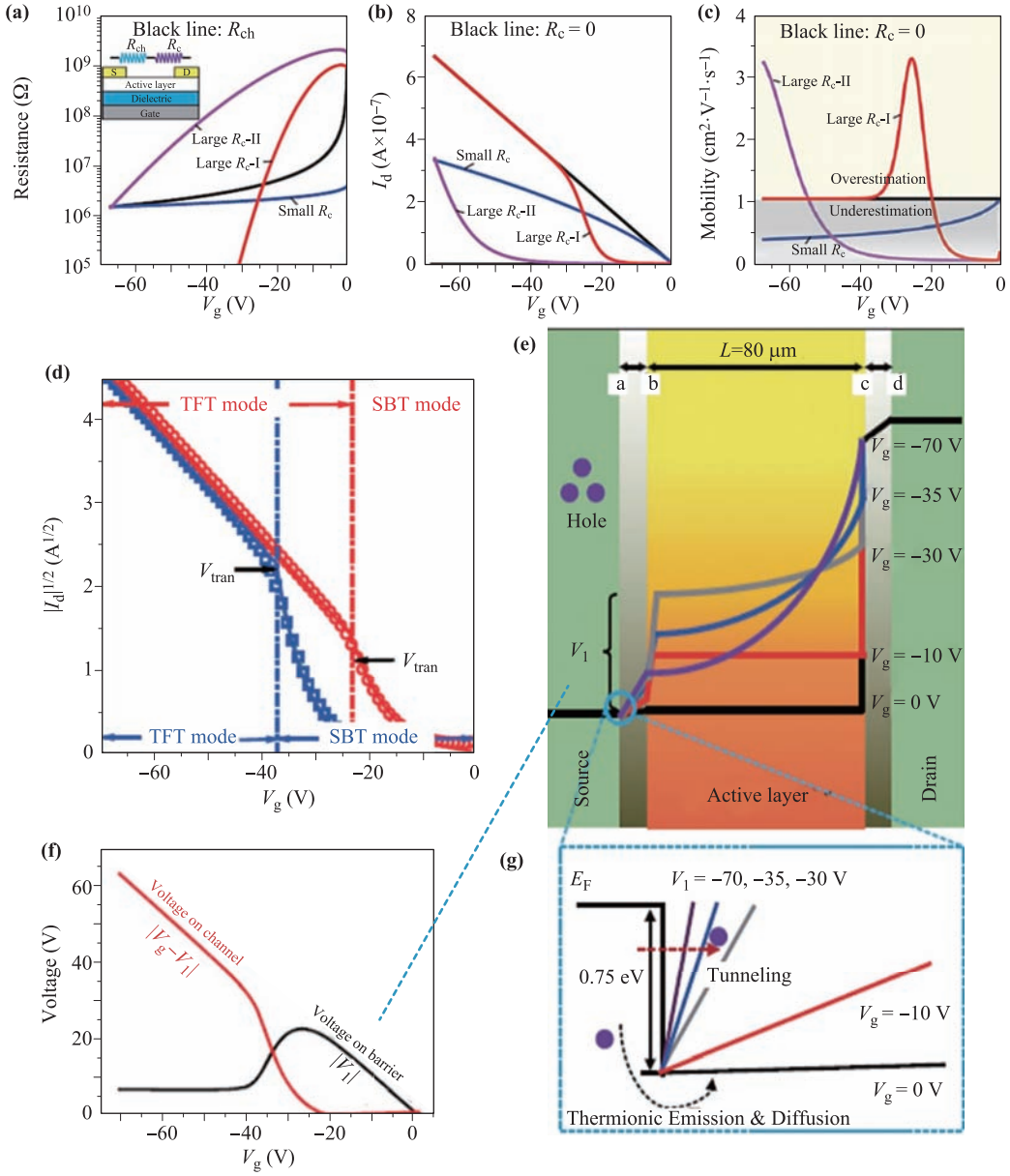


Fig. 2 **(a–c)** The varying of resistance (a), drain current (b) and mobility (c) at different gate bias in linear regime; **(d)** The devices work in different mode (Schottky mode, MOSFET mode or transition mode); **(e)** The effect of gate bias on the valence band in the band diagram; **(f)** Voltage distribution in the contact region and channel region; **(g)** Injection from source electrodes to active layer, and the valance band near the electrode at different gate bias. Reproduced from Ref. [57].

3 Strategies for reducing the nonideal behaviors

3.1 Doping and molecular engineering

Based on the previous discussions, we now have a preliminary idea of the origin of the nonideal double-slope effect. According to the results discussed in Section 2.2, charge trapping effect is likely to induce nonideal double-slope behaviors, especially for D-A polymers. As for these polymers, the active functional groups, gate bias, a trace amount of water trapped in the semiconductors and oxygen play important roles in charge trapping progress, and the electrons are continuously injected and accumulated in the charge transport channel. According to this reasoning, ideal p-type OFETs can be realized by suppressing the injection and accumulation of electrons. Recently, it has been shown that doping semiconductors can effectively improve the performance of OFETs and is beneficial to suppress the nonideal double-slope behaviors [55, 70–79]. Bazan *et al.* reported that the nonideal double-slope behaviors could be suppressed by doping PCBM in D-A polymer semiconductors [76]. As shown in Fig. 5(a), the

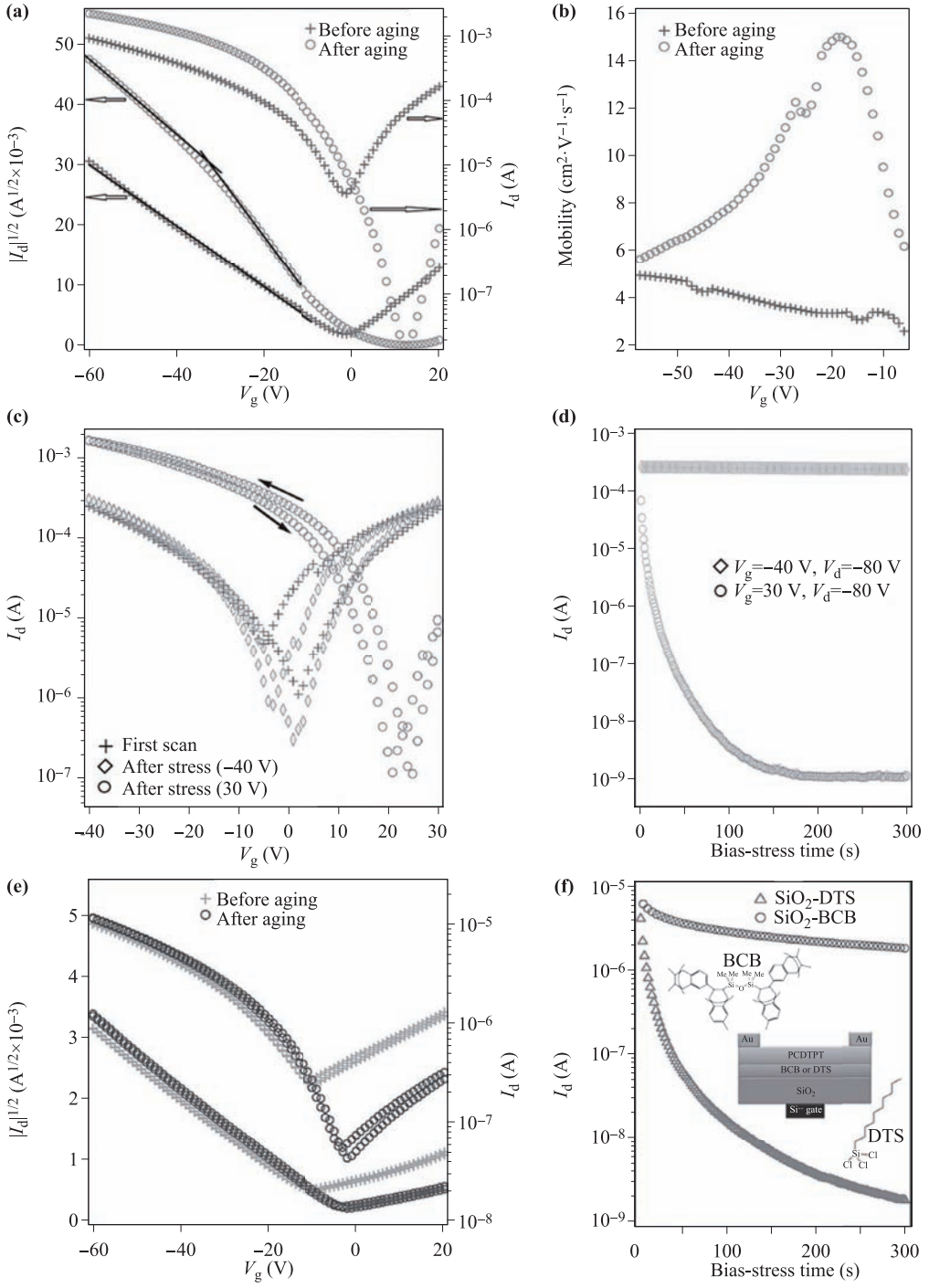


Fig. 3 **(a)** Transfer characteristics of the OFET before and after aging; **(b)** Mobility at different gate bias before and after aging; **(c)** The transfer characteristics before and after stressing at different gate bias; **(d)** Drain-current decay after stressing in the hole conduction ($V_g = -40$ V) and the electron conduction ($V_g = +30$ V) regime; **(e)** Transfer characteristics of the BCB device before and after stressing; **(f)** Drain current decay of device with and without BCB. Reproduced from Ref. [48].

device had shown obvious double-slope behaviors after being operated by bias-sweeping through 100 cycles. However, ideal transfer characteristics could be observed by using the PCBM additive into the D-A polymer [Fig. 5(b)]. With the introduction of PCBM, the electrons are tightly bound at the fullerene sites and impeded from accumulating and trapping at the dielectric/semiconductor interface, resulting in ideal OFETs. Similarly, Chan *et al.* proposed that the nonideal double-slope behaviors could be effectively suppressed by using surface doping, as shown in Figs. 5(c)–(e) [79]. The doped F4-TCNQ can diffuse into the contact and channel region, which is beneficial for

injection and transport of carriers [Fig. 5(e)]. From the energy band diagram, F4-TCNQ is mainly related to the trap filling process in the bandgap, which is triggered by the spontaneous charge transfer at the interface between F4-TCNQ and semiconductor [Fig. 5(d)].

Apart from the surface or internal doping of the semiconductor layer, ideal p-type OFETs can be realized by molecular engineering [80–83], to inhibit the electron injection and accumulation process. The LUMO level is associated with electron injection and ambipolarity in the semiconductors. Therefore, the electrical stability of the devices can be improved by adjusting the LUMO level. Bazan *et al.* reported that electron injection can be suppressed by introducing the units with low electron withdrawing abilities (Fig. 6) [83]. From the UV-vis absorption spectrum and cyclic voltammetry curve, the LUMO

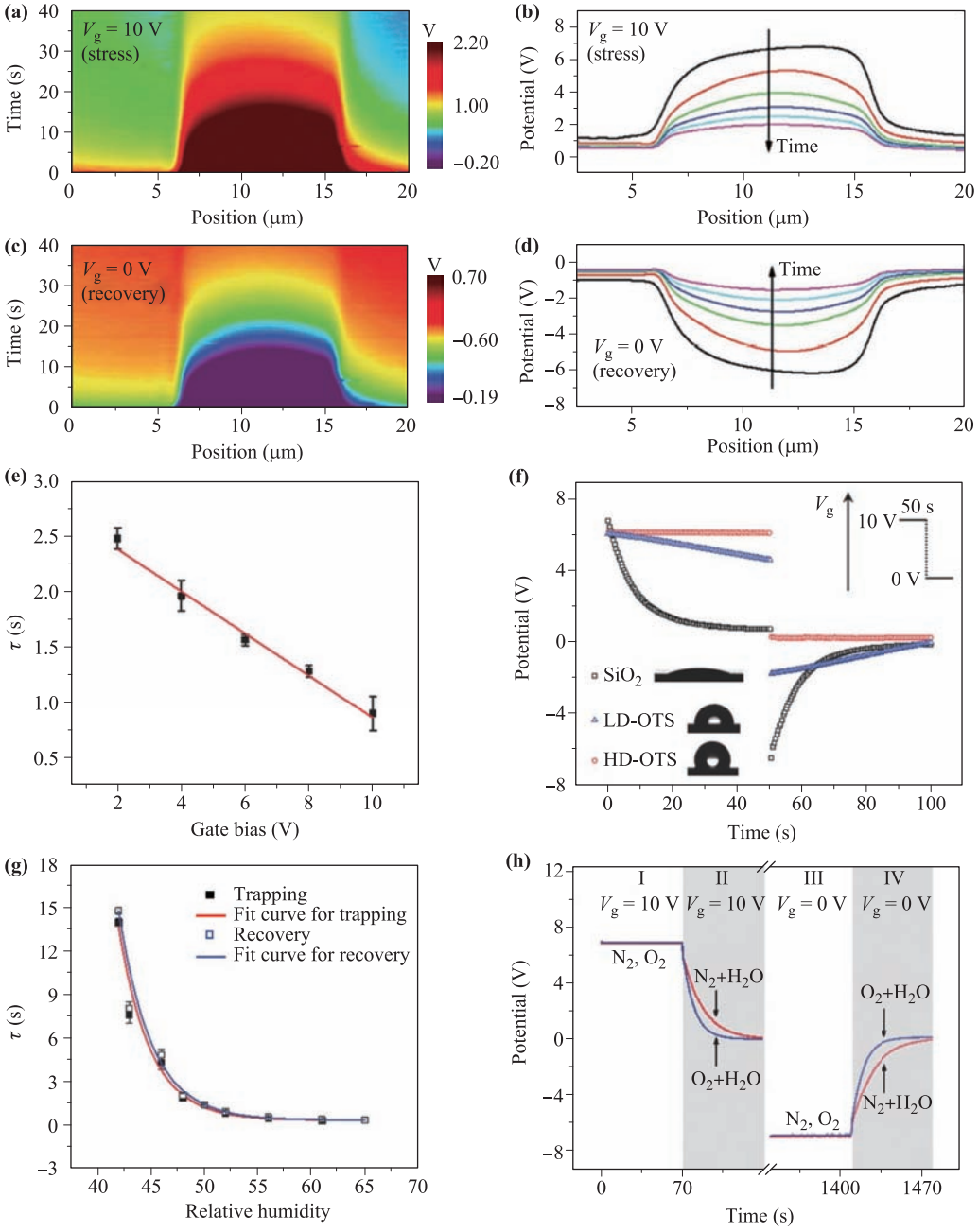


Fig. 4 **(a)** Potential distribution of the $n^{++}Si/SiO_2/Au$ substrate at V_g = 10 V; **(b)** The potential varies with time extracted from (a); **(c, d)** Results at V_g = 0 V; **(e)** The recovery time of the channel potential at different gate bias; **(f)** Evolutions of potential in channel region for substrates with different density OTS SAMs; **(g)** The recovery time of the channel potential at different relative humidity; **(h)** The attenuation and recovery of channel potentials under different environments. Reproduced from Ref. [6].

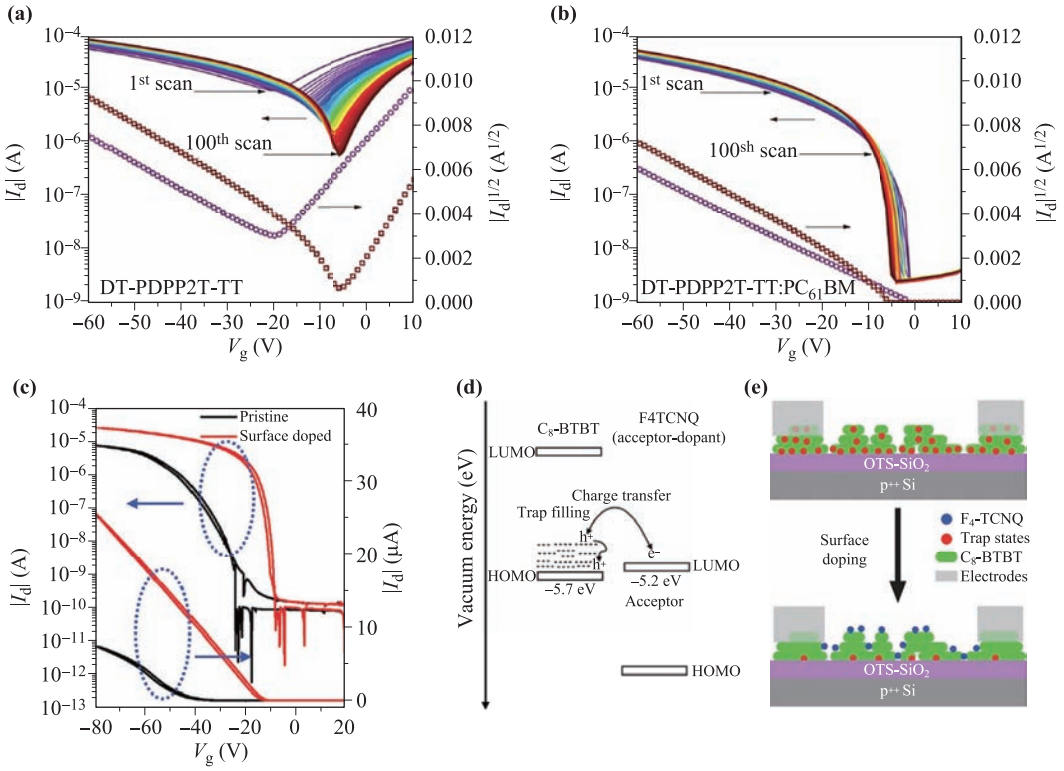


Fig. 5 **(a, b)** Transfer characteristics under 100 scans for OFETs based on DT-PDPP2T-TT films and DT-PDPP2T-TT:PCBM films. Reproduced from Ref. [76]. **(c)** Transfer characteristics of pristine an d surface doped OFETs; **(d)** Energy band diagram of the F4-TCNQ surface doped C_8-BTBT, showing the charge transfer process; **(e)** The trap states evolution process before and after surface doping. Reproduced from Ref. [79].

levels were estimated, with values of −3.0 eV for PhF0, −3.1 eV for PhF1 and −3.3 eV for PhF2,5 [Figs. 6(b) and (c)]. The OFETs based on these polymers with different LUMO levels were fabricated with bottom-gate bottom-contact (BGBC) architecture. As can be seen in the transfer characteristics, the polymer PhF2,5 exhibits ideal be-

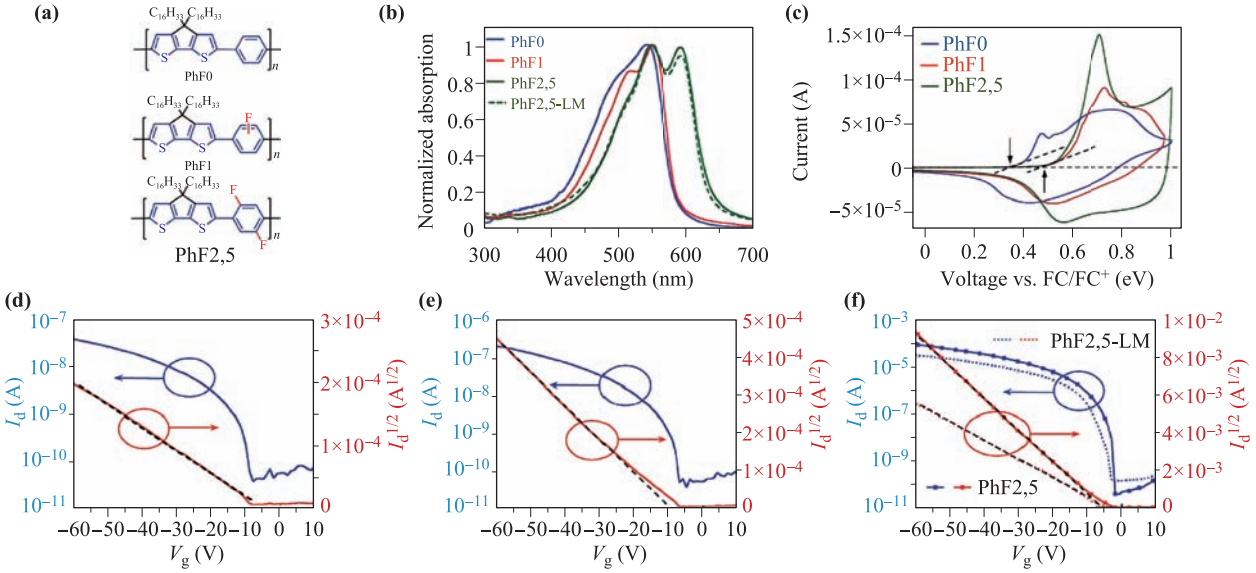


Fig. 6 **(a)** Chemical structures of PhF0, PhF1 and PhF2,5; **(b, c)** UV-vis absorption spectrum and cyclic voltammetry curves of thin films; **(d–f)** Transfer characteristics of PhF0, PhF1 and PhF2,5 films. Reproduced from Ref. [83].

haviors after bias-sweeping [Figs. 6(d)–(f)].

3.2 Reducing charge trapping

Due to its surface flatness, stability and scalable production, SiO_2 is an ideal dielectric layer for commercial use. However, with the development of performance of OFETs, the application of this dielectric layer has run into difficulties, which arises from the large number of traps at the surface. To deal with this problem, trap passivation with self-assembled monolayers (SAMs) is usually carried out to improve the surface of SiO_2, which can significantly enhance the performance of OFETs [19, 37, 43, 45, 48, 84–86]. Nevertheless, the surface of SiO_2 is difficult to be completely covered or passivated, and the charge trapping process still happens even on the high-density SAM-modified SiO_2 surface, which induces the nonideal double-slope behaviors [6].

Some strategies for reducing interface charge trapping have been proposed. Yu *et al.* demonstrated that the polymer (PAIID-BT-C_1) devices exhibited nonideal double-slope and unipolar transporting behaviors when measured at BGBC configuration [Fig. 7(a)] [87]. The devices show the highest hole mobility of 3.63 $cm^2 \cdot V^{-1} \cdot s^{-1}$. The ambipolar and almost ideal OFET behaviors have been observed when they were fabricated in top-gate bottom-contact (TGBC) configuration with PMMA as the dielectric layer [Fig. 7(b)]. However, much reduced mobility was obtained, with the hole and electron mobilities being 0.45 and 0.47 $cm^2 \cdot V^{-1} \cdot s^{-1}$, respectively. Similarly, Nguyen *et al.* realized OFETs with ideal transfer characteristics by inserting an insulating layer (BCB) with lower defect density between SiO_2 and the semiconductor layer. The BCB was selected as the inserting layer for preventing the absorption of water and reducing the charge trapping [Fig. 3(e)] [48]. Sirringhaus *et al.* demonstrated that the nonideal double-slope phenomenon could be avoided by dipping the IDTBT (indacenodithiophene-co-benzothiadiazole) films into acetonitrile solvent [Figs. 7(d)–(f)] [88]. All the devices exhibit ideal characteristics with gate bias independent mobility of 3 $cm^2 \cdot V^{-1} \cdot s^{-1}$. This is because the acetonitrile solvent could form azeotropes with water, which reduces the effect of water on charge trapping process. These results demonstrate that the ideal characteristics of OFETs can be obtained by reducing the trapping of charge carriers at the semiconductor/dielectric interface or in the semiconductor bulk.

3.3 Contact engineering

As discussed above, contact resistance could induce the nonideal double-slope behaviors. So, reducing contact resistance or realizing Ohmic contacts can be an effective method for removing double-slope effect. There are several strategies to improve the carrier injection efficiency and to lower contact resistance, such as modifying the electrodes by SAMs, utilizing monolayer semiconductors, post-annealing treatment of semiconductors or inserting a charge injection layer [23, 30, 89–99]. Porter *et al.* reported the effect of SAMs on charge injection and transport in poly(3-hexylthiophene)-based OFETs [Figs. 8(a) and (b)] [91]. They demonstrated that the metal work function could be regulated by treating with

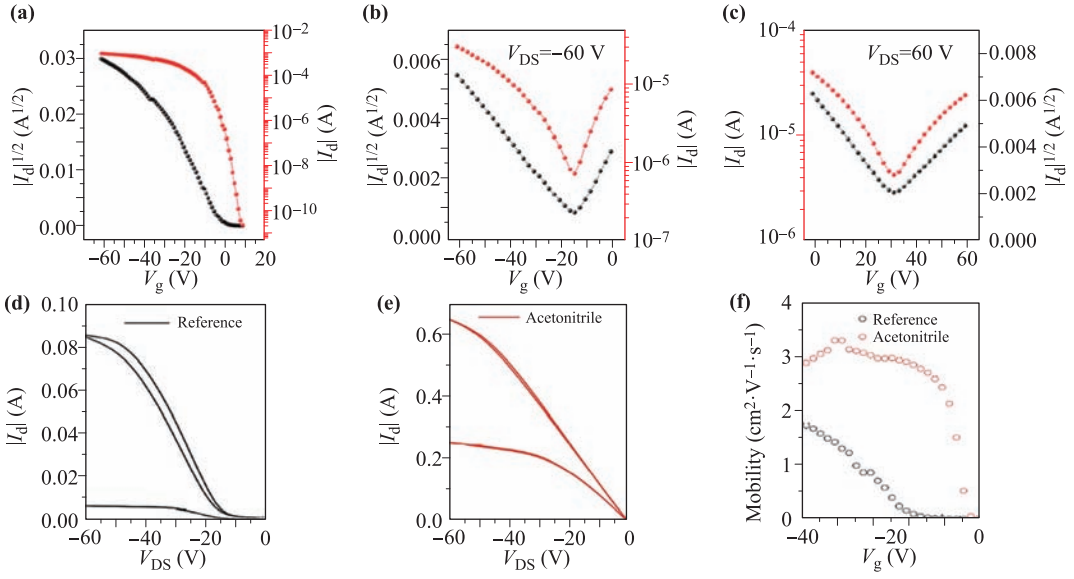


Fig. 7 **(a)** Transfer characteristics of OFETs with BGBC configuration; **(b, c)** Transfer characteristics of OFETs with TGBC configuration. Reproduced from Ref. [87]. **(d)** Output characteristics for IDTBT OFET; **(e)** Output characteristics for a reference device after acetonitrile treated; **(f)** Gate-voltage dependence of the extracted mobility for IDTBT devices and acetonitrile treated devices. Reproduced from Ref. [88].

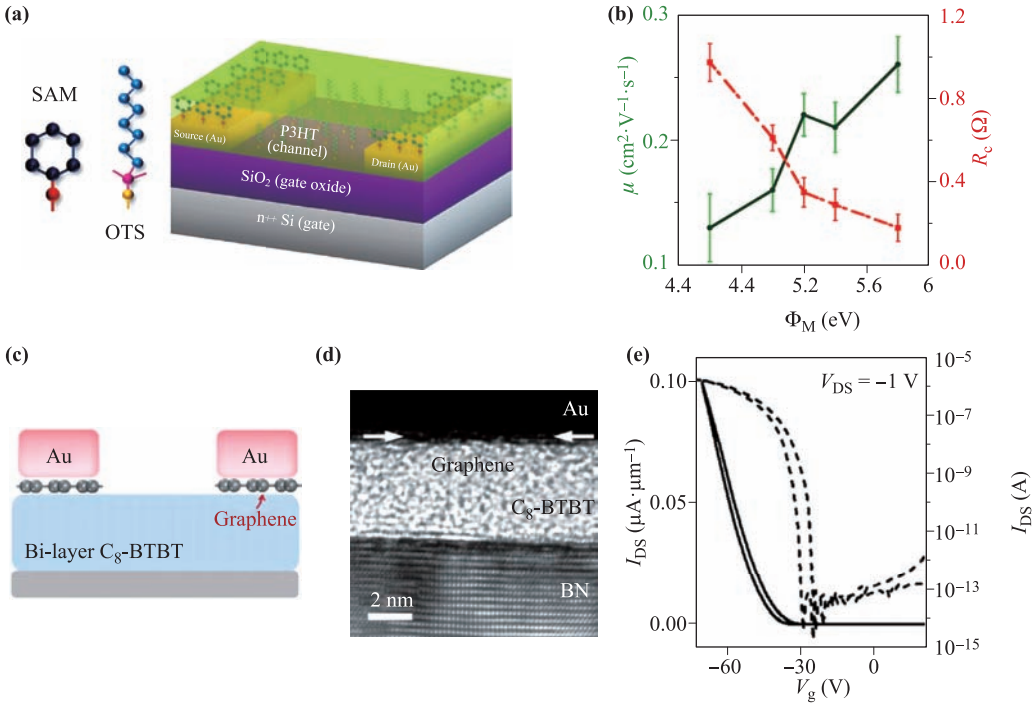


Fig. 8 **(a)** The device structure diagram with the SAM layer on electrodes; **(b)** The contact work function dependence of mobility and contact resistance. Reproduced from Ref. [91]. **(c)** Schematic diagram of the device; **(d)** Cross-sectional TEM image of contact region; **(e)** Transfer characteristics of graphene-contacted device. Reproduced from Ref. [89].

different SAMs, which affected the charge injection process. The charge injection process is closely related to the contact resistance and mobility. The contact resistance decreased from 0.61 MΩ for untreated electrodes to 0.18 MΩ for SAM-treated electrodes [Fig. 8(b)]. At the same time, the mobility increased from 0.16 $cm^2 \cdot V^{-1} \cdot s^{-1}$ to 0.26 $cm^2 \cdot V^{-1} \cdot s^{-1}$. The change in the work function of the metal electrodes also affects the gate dependence of the contact resistance, which is beneficial to obtain ideal electrical characteristics of devices.

Similarly, Takeya *et al.* demonstrated that the nonideal behaviors could be eliminated effectively by annealing the semiconductors, which the contact resistance reached 200 Ω·cm [99]. Jurchescu *et al.* reported the enhance performance of OFETs through modification of the contact deposition rate in both small molecule and polymer semiconductors. They found that by lower the deposition rate of Au contacts, high work function domains can be produced at the surface of the injection electrodes, which can promote charge injection to achieve a contact resistance as low as 200 Ω·cm [100]. Wang *et al.* also reported that contact resistance can be significantly reduced by inserting a doped graphene between the C8BTBT and electrodes [Figs. 8(c)–(e)] [89]. As shown in Figs. 8(c) and (d), the BGTC configuration OFETs with doped graphene/Au stack as the contact were studied systematically. The transfer characteristics exhibited ideal behaviors with a mobility of 2–4 $cm^2 \cdot V^{-1} \cdot s^{-1}$ [Fig. 8(e)]. These results demonstrated that the nonideal double-slope characteristics can be eliminated by improving the charge injection efficiency. In fact, there are many other viable methods to reduce contact resistance in OFETs by contact engineering, and have been well summarized in previous reviews [55, 62].

4 Utilizations of nonideal OFETs

Although we have made great progress in fabricating OFETs with high mobility, the emergence of nonideal double-slope characteristics makes it difficult to describe the electrical behaviors of these OFETs with classical MOSFET model, and also is unfavorable for the application of OFETs. However, it does not mean that the nonideal double-slope characteristics are useless. Generally, the nonideal OFETs have large contact resistance (Schottky contacts) or serious trapping effects. We can utilize these features for special applications through the strategies of interface engineering, contact engineering and molecular designing [101–106]. In fact, it is a common method to develop the high-performance optical memory devices by taking the advantages of intrinsic trap states. Li's group demonstrated the high-performance memory devices realized by growing single crystals of ferroelectric organometal halide perovskite on C_{60} single crystals (Fig. 9) [103]. As shown in Figs. 9(a) and (b), the FETs

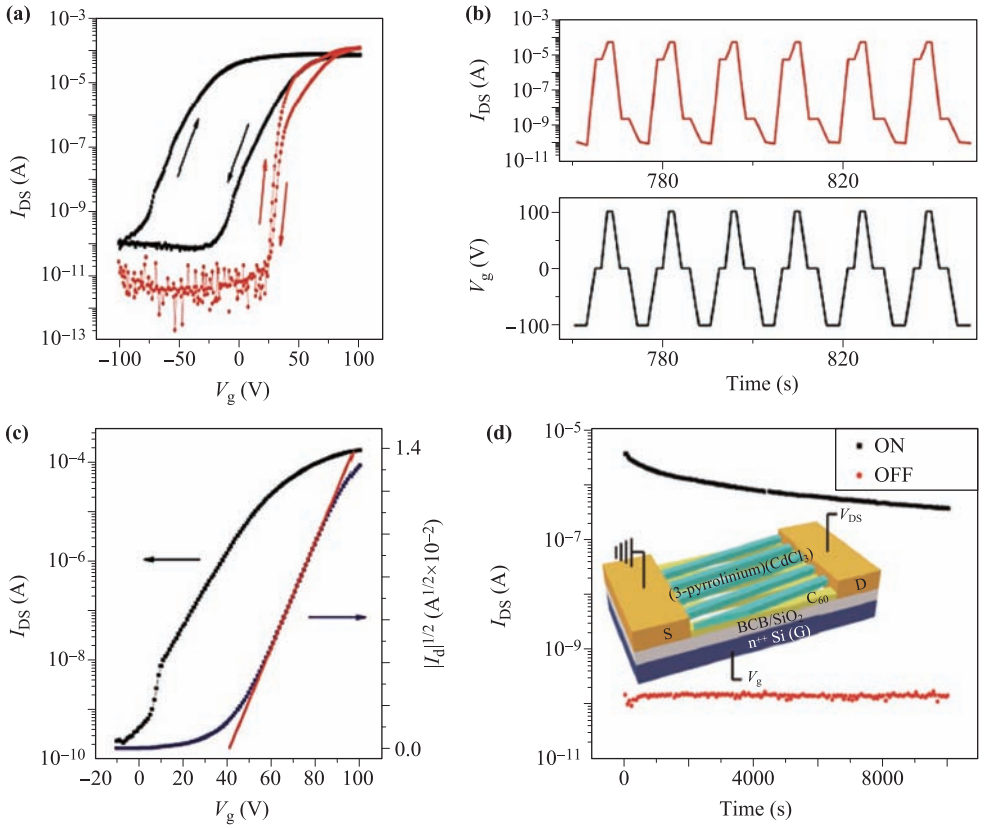


Fig. 9 **(a)** The hysteresis characteristics of FETs based on C_{60} crystals with and without (3-pyrrolinium) ($CdCl_3$) crystals; **(b)** Transfer characteristics of the OFETs; **(c, d)** WRER cycles and retention time test of the memory devices. Reproduced from Ref. [103].

based on $CdCl_3/C_{60}$ crystals exhibit a large threshold shift and hysteresis as well, which is beneficial for organic memory devices. The memory devices show a good endurance characteristics and long retention time of at least 10^4 s [Fig. 9(c) and (d)]. The efficient combination of ferroelectric monocrystals and organic semiconductor monocrystals provides a simple method to fabricate high performance memory devices. In addition, the nonideal Schottky contacts can also be used to fabricate large-gain inverters [101]. Moreover, OFET-based photo-stimulated synapse emulators have been reported by utilizing the traps at the interface between the semiconductors and dielectrics [107]. All these works show that the nonideal effects in OFETs, although may not be favorable for obtaining high-performance OFETs, may still be useful in some specific applications.

5 Conclusions and outlook

In summary, with the development of OFET performance, the nonideal double-slope characteristics have been widely observed. The nonideal characteristics make it difficult to calculate the intrinsic performance of devices. This review summarized and discussed several possible mechanisms to explain the origin of nonideal double-slope behaviors, including contact resistance effects, charge trapping effects, disorder effects and coulombic interactions. Although great progress has been made on understanding the nonideal double-slope effects, we have not achieved a unified mechanism to explain the nonideal phenomenon. However, by these studies and investigations, we have been able to introduce several strategies to remove or mitigate the nonideal behaviors OFETs. For example, we can use doping and molecular engineering to inhibit the electron injection and accumulation. Contact engineering and trap passivation can also be employed to improve the injection efficiency of carriers and reduce the density of interface defect states, respectively. The knowledge about double-slope effect and the strategies that can be employed for removing this effect presented in this review can be important to proper analysis of OFET performance and to the application of them as well. Furthermore, these nonideal double-slope effects can also be applied in other special devices, such as large gain inverters by utilizing Schottky contacts and memory devices by utilizing trapping states.

Acknowledgements This work was supported by the Ministry of Science and Technology of China (Grant No. 2017YFA0204704), the National Natural Science Foundation of China (Grant Nos. 21873108

and 21805284), the Chinese Academy of Sciences (Hundred Talents Plan), and the Strategic Priority Research Program (Grant No. XDB30000000).

References

1. H. Klauk, U. Zschieschang, J. Pflaum, and M. Halik, Ultralow-power organic complementary circuits, *Nature* 445(7129), 745 (2007)
2. G. Gelinck, P. Heremans, K. Nomoto, and T. D. Anthopoulos, Organic transistors in optical displays and microelectronic applications, *Adv. Mater.* 22(34), 3778 (2010)
3. C. Zhang, P. Chen, and W. Hu, Organic field-effect transistor-based gas sensors, *Chem. Soc. Rev.* 44(8), 2087 (2015)
4. J. Y. Oh, S. Rondeau-Gagne, Y. C. Chiu, A. Chortos, F. Lissel, G. N. Wang, B. C. Schroeder, T. Kurosawa, J. Lopez, T. Katsumata, J. Xu, C. Zhu, X. Gu, W. G. Bae, Y. Kim, L. Jin, J. W. Chung, J. B. Tok, and Z. Bao, Intrinsically stretchable and healable semiconducting polymer for organic transistors, *Nature* 539(7629), 411 (2016)
5. Y. Zang, D. Huang, C. A. Di, and D. Zhu, Device engineered organic transistors for flexible sensing applications, *Adv. Mater.* 28(22), 4549 (2016)
6. H. I. Un, P. Cheng, T. Lei, C. Y. Yang, J. Y. Wang, and J. Pei, Charge-trapping-induced non-ideal behaviors in organic field-effect transistors, *Adv. Mater.* 30(18), 1800017 (2018)
7. R. Warren, A. Privitera, P. Kaienburg, A. E. Lauritzen, O. Thimm, J. Nelson, and M. K. Riede, Controlling energy levels and Fermi level en route to fully tailored energetics in organic semiconductors, *Nat. Commun.* 10(1), 5538 (2019)
8. J. Ko, Y. Kim, J. S. Kang, R. Berger, H. Yoon, and K. Char, Enhanced vertical charge transport of homo- and blended semiconducting polymers by nanoconfinement, *Adv. Mater.* 32(10), 1908087 (2020)
9. G. Schweicher, G. Garbay, R. Jouclas, F. Vibert, F. Devaux, and Y. H. Geerts, Molecular semiconductors for logic operations: Dead-end or bright future? *Adv. Mater.* 32(10), 1905909 (2020)
10. X. Wang, R. Kerr, F. Chen, N. Goujon, J. M. Pringle, D. Mecerreyes, M. Forsyth, and P. C. Howlett, Toward high-energy-density lithium metal batteries: Opportunities and challenges for solid organic electrolytes, *Adv. Mater.* 32(18), 1905219 (2020)
11. H. Fukagawa, M. Hasegawa, K. Morii, K. Suzuki, T. Sasaki, and T. Shimizu, Universal strategy for efficient electron injection into organic semiconductors utilizing hydrogen bonds, *Adv. Mater.* 31(43), 1904201 (2019)
12. Y. Li, C. Ji, Y. Qu, X. Huang, S. Hou, C. Z. Li, L. S. Liao, L. J. Cuo, and S. R. Forrest, Enhanced light utilization in semitransparent organic photovoltaics using an optical outcoupling architecture, *Adv. Mater.* 31(40), 1903173 (2019)
13. J. Mun, J. Kang, Y. Zheng, S. Luo, H. C. Wu, N. Matsuhisa, J. Xu, G. N. Wang, Y. Yun, G. Xue, J. B. H. Tok, and Z. Bao, Conjugated carbon cyclic nanorings as additives for intrinsically stretchable semiconducting polymers, *Adv. Mater.* 31(42), 1903912 (2019)
14. Y. Yamashita, J. Tsurumi, M. Ohno, R. Fujimoto, S. Kumagai, T. Kurosawa, T. Okamoto, J. Takeya, and S. Watanabe, Efficient molecular doping of polymeric semiconductors driven by anion exchange, *Nature* 572(7771), 634 (2019)
15. J. Xu, S. Wang, G. N. Wang, C. Zhu, S. Luo, L. Jin, X. Gu, S. Chen, V. R. Feig, J. W. To, S. Rondeau-Gagne, J. Park, B. C. Schroeder, C. Lu, J. Y. Oh, Y. Wang, Y. H. Kim, H. Yan, R. Sinclair, D. Zhou, G. Xue, B. Murmann, C. Linder, W. Cai, J. B. Tok, J. W. Chung, and Z. Bao, Highly stretchable polymer semiconductor films through the nanoconfinement effect, *Science* 355(6320), 59 (2017)
16. P. Chao, H. Chen, Y. Zhu, H. Lai, D. Mo, N. Zheng, X. Chang, H. Meng, F. He, and A. Benzo, [1,2-b:4,5-c]dithiophene-4,8-dione-based polymer donor achieving an efficiency over 16%, *Adv. Mater.* 32(10), 1907059 (2020)
17. Y. Gao, Y. Yi, X. Wang, H. Meng, D. Lei, X. F. Yu, P. K. Chu, and J. Li, A novel hybrid-layered organic phototransistor enables efficient intermolecular charge transfer and carrier transport for ultrasensitive photodetection, *Adv. Mater.* 31(16), 1900763 (2019)
18. J. Wang, H. Yu, T. Fu, C. Zhao, H. Yu, Z. Liu, Q. He, D. Zhang, H. Meng, and W. Huang, Wide band gap pyromellitic diimides for photo stable *n*-channel thin film transistors, *J. Mater. Chem. C* 8(22), 7344 (2020)
19. X. Ren, F. Yang, X. Gao, S. Cheng, X. Zhang, H. Dong, and W. Hu, Organic field-effect transistor for energy-related applications: Low-power-consumption devices, near-infrared phototransistors, and organic thermoelectric devices, *Adv. Energy Mater.* 8(24), 1801003 (2018)
20. T. N. Jackson, Y.-Y. Lin, D. J. Gundlach, and H. Klauk, Organic thin-film transistors for organic light-emitting flat-panel display backplanes, *IEEE J. Sel. Top. Quantum Electron.* 4(1), 100 (1998)
21. P. F. Baude, D. A. Ender, M. A. Haase, T. W. Kelley, D. V. Muyres, and S. D. Theiss, Pentacene-based radio-frequency identification circuitry, *Appl. Phys. Lett.* 82(22), 3964 (2003)
22. Y. Yao, H. Dong, and W. Hu, Charge transport in organic and polymeric semiconductors for flexible and stretchable devices, *Adv. Mater.* 28(22), 4513 (2016)
23. H. Li, Y. Shi, G. Han, J. Liu, J. Zhang, C. Li, J. Liu, Y. Yi, T. Li, X. Gao, C. Di, J. Huang, Y. Che, D. Wang, W. Hu, Y. Liu, and L. Jiang, Monolayer two-dimensional molecular crystals for an ultrasensitive OFET-based chemical sensor, *Angew. Chem. Int. Ed.* 59(11), 4380 (2020)
24. I. Yagi, N. Hirai, Y. Miyamoto, M. Noda, A. Imaoka, N. Yoneya, K. Nomoto, J. Kasahara, A. Yumoto, and T. Urabe, A flexible full-color AMOLED display driven by OTFTs, *J. Soc. Inf. Disp.* 16(1), 15 (2008)

25. C. Reese, and Z. Bao, Detailed characterization of contact resistance, gate-bias-dependent field-effect mobility, and short-channel effects with microscale elastomeric single-crystal field-effect transistors, *Adv. Funct. Mater.* 19(5), 763 (2009)
26. W. Deng, X. Zhang, C. Gong, Q. Zhang, Y. Xing, Y. Wu, X. Zhang, and J. Jie, Aligned nanowire arrays on thin flexible substrates for organic transistors with high bending stability, *J. Mater. Chem. C* 2(7), 1314 (2014)
27. C. Wang, H. Dong, L. Jiang, and W. Hu, Organic semiconductor crystals, *Chem. Soc. Rev.* 47(2), 422 (2018)
28. K. Ryu, I. Kymissis, V. Bulovic, and C. G. Sodini, Direct extraction of mobility in pentacene OFETs using C–V and I–V measurements, *IEEE Electron Device Lett.* 26(10), 716 (2005)
29. E. G. Bittle, J. I. Basham, T. N. Jackson, O. D. Jurchescu, and D. J. Gundlach, Mobility overestimation due to gated contacts in organic field-effect transistors, *Nat. Commun.* 7(1), 10908 (2016)
30. Y. Shi, L. Jiang, J. Liu, Z. Tu, Y. Hu, Q. Wu, Y. Yi, E. Gann, C. R. McNeill, H. Li, W. Hu, D. Zhu, and H. Sirringhaus, Bottom-up growth of *n*-type monolayer molecular crystals on polymeric substrate for optoelectronic device applications, *Nat. Commun.* 9(1), 2933 (2018)
31. Q. Tang, H. Li, Y. Liu, and W. Hu, High-performance air-stable *n*-type transistors with an asymmetrical device configuration based on organic single-crystalline submicrometer/nanometer ribbons, *J. Am. Chem. Soc.* 128(45), 14634 (2006)
32. J. H. Gao, R. J. Li, L. Q. Li, Q. Meng, H. Jiang, H. X. Li, and W. P. Hu, High-performance field-effect transistor based on dibenzo[d,d]thieno[3,2-b;4,5-b]dithiophene, an easily synthesized semiconductor with high ionization potential, *Adv. Mater.* 19(19), 3008 (2007)
33. J. Takeya, M. Yamagishi, Y. Tominari, R. Hirahara, Y. Nakazawa, T. Nishikawa, T. Kawase, T. Shimoda, and S. Ogawa, Very high-mobility organic single-crystal transistors with in-crystal conduction channels, *Appl. Phys. Lett.* 90(10), 102120 (2007)
34. H. Minemawari, T. Yamada, H. Matsui, J. Tsutsumi, S. Haas, R. Chiba, R. Kumai, and T. Hasegawa, Inkjet printing of single-crystal films, *Nature* 475(7356), 364 (2011)
35. H. R. Tseng, L. Ying, B. B. Hsu, L. A. Perez, C. J. Takacs, G. C. Bazan, and A. J. Heeger, High mobility field effect transistors based on macroscopically oriented regioregular copolymers, *Nano Lett.* 12(12), 6353 (2012)
36. C. Luo, A. K. Kyaw, L. A. Perez, S. Patel, M. Wang, B. Grimm, G. C. Bazan, E. J. Kramer, and A. J. Heeger, General strategy for self-assembly of highly oriented nanocrystalline semiconducting polymers with high mobility, *Nano Lett.* 14(5), 2764 (2014)
37. H. R. Tseng, H. Phan, C. Luo, M. Wang, L. A. Perez, S. N. Patel, L. Ying, E. J. Kramer, T. Q. Nguyen, G. C. Bazan, and A. J. Heeger, High-mobility field-effect transistors fabricated with macroscopic aligned semiconducting polymers, *Adv. Mater.* 26(19), 2993 (2014)
38. Y. Yuan, G. Giri, A. L. Ayzner, A. P. Zoombelt, S. C. Mannsfeld, J. Chen, D. Nordlund, M. F. Toney, J. Huang, and Z. Bao, Ultra-high mobility transparent organic thin film transistors grown by an off-centre spin-coating method, *Nat. Commun.* 5(1), 3005 (2014)
39. J. H. Dou, Y. Q. Zheng, Z. F. Yao, T. Lei, X. Shen, X. Y. Luo, Z. A. Yu, S. D. Zhang, G. Han, Z. Wang, Y. Yi, J. Y. Wang, and J. Pei, A cofacially stacked electron-deficient small molecule with a high electron mobility of over 10 $cm^2 \cdot V^{-1} \cdot s^{-1}$ in air, *Adv. Mater.* 27(48), 8051 (2015)
40. J. Liu, H. Zhang, H. Dong, L. Meng, L. Jiang, L. Jiang, Y. Wang, J. Yu, Y. Sun, W. Hu, and A. J. Heeger, High mobility emissive organic semiconductor, *Nat. Commun.* 6(1), 10032 (2015)
41. Y. Q. Zheng, T. Lei, J. H. Dou, X. Xia, J. Y. Wang, C. J. Liu, and J. Pei, Strong electron-deficient polymers lead to high electron mobility in air and their morphology-dependent transport behaviors, *Adv. Mater.* 28(33), 7213 (2016)
42. G. Giri, E. Verploegen, S. C. B. Mannsfeld, S. Atahan-Evrenk, D. H. Kim, S. Y. Lee, H. A. Becerril, A. Aspuru-Guzik, M. F. Toney, and Z. Bao, Tuning charge transport in solution-sheared organic semiconductors using lattice strain, *Nature* 480(7378), 504 (2011)
43. H. Chen, Y. Guo, G. Yu, Y. Zhao, J. Zhang, D. Gao, H. Liu, and Y. Liu, Highly pi-extended copolymers with diketopyrrolopyrrole moieties for high-performance field-effect transistors, *Adv. Mater.* 24(34), 4618 (2012)
44. J. Li, Y. Zhao, H. S. Tan, Y. Guo, C. A. Di, G. Yu, Y. Liu, M. Lin, S. H. Lim, Y. Zhou, H. Su, and B. S. Ong, A stable solution-processed polymer semiconductor with record high-mobility for printed transistors, *Sci. Rep.* 2(1), 754 (2012)
45. I. Kang, T. K. An, J. A. Hong, H. J. Yun, R. Kim, D. S. Chung, C. E. Park, Y. H. Kim, and S. K. Kwon, Effect of selenophene in a DPP copolymer incorporating a vinyl group for high-performance organic field-effect transistors, *Adv. Mater.* 25(4), 524 (2013)
46. H. Sirringhaus, 25th anniversary article: Organic field-effect transistors: The path beyond amorphous silicon, *Adv. Mater.* 26(9), 1319 (2014)
47. S. Fratini, H. Xie, I. N. Hulea, S. Ciuchi, and A. F. Morpurgo, Current saturation and Coulomb interactions in organic single-crystal transistors, *New J. Phys.* 10(3), 033031 (2008)
48. H. Phan, M. Wang, G. C. Bazan, and T. Q. Nguyen, Electrical instability induced by electron trapping in low-bandgap donor-acceptor polymer field-effect transistors, *Adv. Mater.* 27(43), 7004 (2015)
49. Y. Xu, T. Minari, K. Tsukagoshi, J. A. Chroboczek, and G. Ghibaudo, Direct evaluation of low-field mobility and access resistance in pentacene field-effect transistors, *J. Appl. Phys.* 107(11), 114507 (2010)
50. F. Chiarella, M. Barra, A. Carella, L. Parlato, E. Sarnelli, and A. Cassinese, Contact-resistance effects in PDI_8-CN_2 n-type thin-film transistors investigated by Kelvin-probe potentiometry, *Org. Electron.* 28, 299 (2016)

51. A. Ablat, A. Kyndiah, G. Houin, T. Y. Alic, L. Hirsch, and M. Abbas, Role of oxide/metal bilayer electrodes in solution processed organic field effect transistors, *Sci. Rep.* 9(1), 6685 (2019)

52. A. Yamamura, T. Sakon, K. Takahira, T. Wakimoto, M. Sasaki, T. Okamoto, S. Watanabe, and J. Takeya, High-speed organic single-crystal transistor responding to very high frequency band, *Adv. Funct. Mater.* 30(11), 1909501 (2020)

53. N. Tessler and Y. Roichman, Two-dimensional simulation of polymer field-effect transistor, *Appl. Phys. Lett.* 79(18), 2987 (2001)

54. T. J. Richards and H. Sirringhaus, Analysis of the contact resistance in staggered, top-gate organic field-effect transistors, *J. Appl. Phys.* 102(9), 094510 (2007)

55. D. Braga and G. Horowitz, High-performance organic field-effect transistors, *Adv. Mater.* 21(14–15), 1473 (2009)

56. S. Mansouri, M. Mahdouani, A. Oudir, S. Zorai, S. Ben Dkhil, G. Horowitz, and R. Bourguiga, Analytic model for organic thin film transistors (OTFTs): Effect of contact resistances application to the octithiophene, *Eur. Phys. J. Appl. Phys.* 48(3), 30401 (2009)

57. C. Liu, G. Li, R. Di Pietro, J. Huang, Y. Y. Noh, X. Liu, and T. Minari, Device physics of contact issues for the overestimation and underestimation of carrier mobility in field-effect transistors, *Phys. Rev. Appl.* 8(3), 034020 (2017)

58. Y. Hu, G. Li, W. Peng, and Z. Chen, Comparing the gate dependence of contact resistance and channel resistance in organic field-effect transistors for understanding the mobility overestimation issue, *IEEE Electron Device Lett.* 39(3), 421 (2018)

59. Z. A. Lamport, H. F. Haneef, S. Anand, M. Waldrip, and O. D. Jurchescu, Tutorial: Organic field-effect transistors: Materials, structure and operation, *J. Appl. Phys.* 124(7), 071101 (2018)

60. B. H. Hamadani and D. Natelson, Temperature-dependent contact resistances in high-quality polymer field-effect transistors, *Appl. Phys. Lett.* 84(3), 443 (2004)

61. M. A. Reyes-Martinez, A. J. Crosby, and A. L. Briseno, Rubrene crystal field-effect mobility modulation via conducting channel wrinkling, *Nat. Commun.* 6(1), 6948 (2015)

62. T. Yang, Q. Wu, F. Dai, K. Huang, H. Xu, C. Liu, C. Chen, S. Hu, X. Liang, X. Liu, Y. Y. Noh, and C. Liu, Understanding, optimizing, and utilizing nonideal transistors based on organic or organic hybrid semiconductors, *Adv. Funct. Mater.* 30(20), 1903889 (2020)

63. C. Liu, C. Chen, X. Li, S. Hu, C. Liu, K. Huang, F. Dai, B. Zhang, X. Liu, T. Minari, Y. Y. Noh, and J. Chen, A general approach to probe dynamic operation and carrier mobility in field-effect transistors with nonuniform accumulation, *Adv. Funct. Mater.* 29(29), 1901700 (2019)

64. D. F. Figer, An upper limit to the masses of stars, *Nature* 434(7030), 192 (2005)

65. C. M. Aguirre, P. L. Levesque, M. Paillet, F. Lapointe, B. C. St-Antoine, P. Desjardins, and R. Martel, The role of the oxygen/water redox couple in suppressing electron conduction in field-effect transistors, *Adv. Mater.* 21(30), 3087 (2009)

66. P. A. Bobbert, A. Sharma, S. G. Mathijssen, M. Kemerink, and D. M. de Leeuw, Operational stability of organic field-effect transistors, *Adv. Mater.* 24(9), 1146 (2012)

67. F. V. Di Girolamo, F. Ciccullo, M. Barra, A. Carella, and A. Cassinese, Investigation on bias stress effects in n-type PDI_8-CN_2 thin-film transistors, *Org. Electron.* 13(11), 2281 (2012)

68. H. N. Tsao, D. M. Cho, I. Park, M. R. Hansen, A. Mavrinskiy, D. Y. Yoon, R. Graf, W. Pisula, H. W. Spiess, and K. Mullen, Ultrahigh mobility in polymer field-effect transistors by design, *J. Am. Chem. Soc.* 133(8), 2605 (2011)

69. Z. Chen, M. J. Lee, R. Shahid Ashraf, Y. Gu, S. Albert-Seifried, M. Meedom Nielsen, B. Schroeder, T. D. Anthopoulos, M. Heeney, I. McCulloch, and H. Sirringhaus, High-performance ambipolar diketopyrrolopyrrole-thieno[3, 2-b]thiophene copolymer field-effect transistors with balanced hole and electron mobilities, *Adv. Mater.* 24(5), 647 (2012)

70. F. Fujimori, K. Shigeto, T. Hamano, T. Minari, T. Miyadera, K. Tsukagoshi, and Y. Aoyagi, Current transport in short channel top-contact pentacene field-effect transistors investigated with the selective molecular doping technique, *Appl. Phys. Lett.* 90(19), 193507 (2007)

71. T. Minari, T. Miyadera, K. Tsukagoshi, Y. Aoyagi, and H. Ito, Charge injection process in organic field-effect transistors, *Appl. Phys. Lett.* 91(5), 053508 (2007)

72. H. Kleemann, C. Schuenemann, A. A. Zakhidov, M. Riede, B. Lüssem, and K. Leo, Structural phase transition in pentacene caused by molecular doping and its effect on charge carrier mobility, *Org. Electron.* 13(1), 58 (2012)

73. T. Minari, P. Darmawan, C. Liu, Y. Li, Y. Xu, and K. Tsukagoshi, Highly enhanced charge injection in thienoacene-based organic field-effect transistors with chemically doped contact, *Appl. Phys. Lett.* 100(9), 093303 (2012)

74. G. Lu, J. Blakesley, S. Himmelberger, P. Pingel, J. Frisch, I. Lieberwirth, I. Salzmann, M. Oehzelt, R. Di Pietro, A. Salleo, N. Koch, and D. Neher, Moderate doping leads to high performance of semiconductor/insulator polymer blend transistors, *Nat. Commun.* 4(1), 1588 (2013)

75. J. E. Cochran, M. J. N. Junk, A. M. Glaudell, P. L. Miller, J. S. Cowart, M. F. Toney, C. J. Hawker, B. F. Chmelka, and M. L. Chabinyc, Molecular interactions and ordering in electrically doped polymers: Blends of PBTTT and F_4TCNQ, *Macromolecules* 47(19), 6836 (2014)

76. M. J. Ford, M. Wang, H. Phan, T. Q. Nguyen, and G. C. Bazan, Fullerene additives convert ambipolar transport to p-type transport while improving the operational stability of organic thin film transistors, *Adv. Funct. Mater.* 26(25), 4472 (2016)

77. M. Nikolka, I. Nasrallah, B. Rose, M. K. Ravva, K. Broch, A. Sadhanala, D. Harkin, J. Charmet, M. Hurhangee, A. Brown, S. Illig, P. Too, J. Jongman, I. McCulloch, J. L. Bredas, and H. Sirringhaus, High operational and environmental stability of high-mobility conjugated polymer field-effect transistors through the use of molecular additives, *Nat. Mater.* 16(3), 356 (2017)

78. J. Panidi, A. F. Paterson, D. Khim, Z. Fei, Y. Han, L. Tsetseris, G. Vourlias, P. A. Patsalas, M. Heeney, and T. D. Anthopoulos, Remarkable enhancement of the hole mobility in several organic small-molecules, polymers, and small-molecule: Polymer blend transistors by simple admixing of the lewis acid p-dopant $B(C_6F_5)_3$, *Adv. Sci.* 5(1), 1700290 (2018)

79. K. Pei, A. H. Y. Lau, and P. K. L. Chan, Understanding molecular surface doping of large bandgap organic semiconductors and overcoming the contact/access resistance in organic field-effect transistors, *Phys. Chem. Chem. Phys.* 22(13), 7100 (2020)

80. C. R. Newman, C. D. Frisbie, D. A. da Silva Filho, J. L. Brédas, P. C. Ewbank, and K. R. Mann, Introduction to organic thin film transistors and design of n-channel organic semiconductors, *Chem. Mater.* 16(23), 4436 (2004)

81. I. McCulloch, M. Heeney, C. Bailey, K. Genevicius, I. Macdonald, M. Shkunov, D. Sparrowe, S. Tierney, R. Wagner, W. Zhang, M. L. Chabinyc, R. J. Kline, M. D. McGehee, and M. F. Toney, Liquid-crystalline semiconducting polymers with high charge-carrier mobility, *Nat. Mater.* 5(4), 328 (2006)

82. H. Phan, M. J. Ford, A. T. Lill, M. Wang, G. C. Bazan, and T. Q. Nguyen, Electrical double-slope nonideality in organic field-effect transistors, *Adv. Funct. Mater.* 28(17), 1707221 (2018)

83. M. Wang, M. J. Ford, A. T. Lill, H. Phan, T. Q. Nguyen, and G. C. Bazan, Hole mobility and electron injection properties of D-A conjugated copolymers with fluorinated phenylene acceptor units, *Adv. Mater.* 29(7), 1603830 (2017)

84. C. Goldmann, C. Krellner, K. P. Pernstich, S. Haas, D. J. Gundlach, and B. Batlogg, Determination of the interface trap density of rubrene single-crystal field-effect transistors and comparison to the bulk trap density, *J. Appl. Phys.* 99(3), 034507 (2006)

85. J. Kan, Y. Chen, D. Qi, Y. Liu, and J. Jiang, High-performance air-stable ambipolar organic field-effect transistor based on tris(phthalocyaninato) europium(III), *Adv. Mater.* 24(13), 1755 (2012)

86. H. Wang, H. Liu, Q. Zhao, C. Cheng, W. Hu, and Y. Liu, Three-component integrated ultrathin organic photosensors for plastic optoelectronics, *Adv. Mater.* 28(4), 624 (2016)

87. J. Huang, Z. Mao, Z. Chen, D. Gao, C. Wei, W. Zhang, and G. Yu, Diazaisoindigo-based polymers with high-performance charge-transport properties: From computational screening to experimental characterization, *Chem. Mater.* 28(7), 2209 (2016)

88. M. Nikolka, G. Schweicher, J. Armitage, I. Nasrallah, C. Jellett, Z. Guo, M. Hurhangee, A. Sadhanala, I. McCulloch, C. B. Nielsen, and H. Sirringhaus, Performance improvements in conjugated polymer devices by removal of water-induced traps, *Adv. Mater.* 30(36), 1801874 (2018)

89. D. He, J. Qiao, L. Zhang, J. Wang, T. Lan, J. Qian, Y. Li, Y. Shi, Y. Chai, W. Lan, L. K. Ono, Y. Qi, J. B. Xu, W. Ji, and X. Wang, Ultrahigh mobility and efficient charge injection in monolayer organic thin-film transistors on boron nitride, *Sci. Adv.* 3(9), e1701186 (2017)

90. X. Cheng, Y. Y. Noh, J. Wang, M. Tello, J. Frisch, R. P. Blum, A. Vollmer, J. P. Rabe, N. Koch, and H. Sirringhaus, Controlling electron and hole charge injection in ambipolar organic field-effect transistors by self-assembled monolayers, *Adv. Funct. Mater.* 19(15), 2407 (2009)

91. K. A. Singh, T. L. Nelson, J. A. Belot, T. M. Young, N. R. Dhumal, T. Kowalewski, R. D. McCullough, P. Nachimuthu, S. Thevuthasan, and L. M. Porter, Effect of self-assembled monolayers on charge injection and transport in poly(3-hexylthiophene)-based field-effect transistors at different channel length scales, *ACS Appl. Mater. Interfaces* 3(8), 2973 (2011)

92. J. Youn, G. R. Dholakia, H. Huang, J. W. Hennek, A. Facchetti, and T. J. Marks, Influence of Thiol self-assembled monolayer processing on bottom-contact thin-film transistors based on n-type organic semiconductors, *Adv. Funct. Mater.* 22(9), 1856 (2012)

93. S. Chung, M. Jang, S. B. Ji, H. Im, N. Seong, J. Ha, S. K. Kwon, Y. H. Kim, H. Yang, and Y. Hong, Flexible high-performance all-inkjet-printed inverters: Organo-compatible and stable interface engineering, *Adv. Mater.* 25(34), 4773 (2013)

94. C. G. Tang, M. C. Ang, K. K. Choo, V. Keerthi, J. K. Tan, M. N. Syafiqah, T. Kugler, J. H. Burroughes, R. Q. Png, L. L. Chua, and P. K. Ho, Doped polymer semiconductors with ultrahigh and ultralow work functions for ohmic contacts, *Nature* 539(7630), 536 (2016)

95. J. Liu, L. Jiang, J. Shi, C. Li, Y. Shi, J. Tan, H. Li, H. Jiang, Y. Hu, X. Liu, J. Yu, Z. Wei, L. Jiang, and W. Hu, Relieving the photosensitivity of organic field-effect transistors, *Adv. Mater.* 32(4), 1906122 (2020)

96. J. Liu, L. Jiang, W. Hu, Y. Liu, and D. Zhu, Monolayer organic field-effect transistors, *Sci. China Chem.* 62(3), 313 (2019)

97. L. Jiang, J. Liu, Y. Shi, D. Zhu, H. Zhang, Y. Hu, J. Yu, W. Hu, and L. Jiang, Realizing low-voltage operating crystalline monolayer organic field-effect transistors with a low contact resistance, *J. Mater. Chem. C* 7(12), 3436 (2019)

98. L. Jiang, J. Liu, X. Lu, L. Fu, Y. Shi, J. Zhang, X. Zhang, H. Geng, Y. Hu, H. Dong, L. Jiang, J. Yu, and W. Hu, Controllable growth of C_8-BTBT single crystalline microribbon arrays by a limited solvent vapor-assisted crystallization (LSVC) method, *J. Mater. Chem. C* 6(10), 2419 (2018)

99. T. Uemura, C. Rolin, T. H. Ke, P. Fesenko, J. Genoe, P. Heremans, and J. Takeya, On the extraction of charge carrier mobility in high-mobility organic transistors, *Adv. Mater.* 28(1), 151 (2016)

100. Z. A. Lamport, K. J. Barth, H. Lee, E. Gann, S. Engmann, H. Chen, M. Guthold, I. McCulloch, J. E. Anthony, L. J. Richter, D. M. DeLongchamp, and O. D. Jurchescu, A simple and robust approach to reducing contact resistance in organic transistors, *Nat. Commun.* 9(1), 5130 (2018)

101. C. Jiang, H. W. Choi, X. Cheng, H. Ma, D. Hasko, and A. Nathan, Printed subthreshold organic transistors operating at high gain and ultralow power, *Science* 363(6428), 719 (2019)

102. R. A. Sporea, M. J. Trainor, N. D. Young, J. M. Shannon, and S. R. Silva, Source-gated transistors for order-of-magnitude performance improvements in thin-film digital circuits, *Sci. Rep.* 4(1), 4295 (2015)

103. J. Wu, C. Fan, G. Xue, T. Ye, S. Liu, R. Lin, H. Chen, H. L. Xin, R. G. Xiong, and H. Li, Interfacing solution-grown C_{60} and (3-Pyrrolinium)($CdCl_3$) single crystals for high-mobility transistor-based memory devices, *Adv. Mater.* 27(30), 4476 (2015)

104. W. Li, F. Guo, H. Ling, P. Zhang, M. Yi, L. Wang, D. Wu, L. Xie, and W. Huang, High-performance nonvolatile organic field-effect transistor memory based on organic semiconductor heterostructures of pentacene/P13/pentacene as both charge transport and trapping layers, *Adv. Sci.* 4(8), 1700007 (2017)

105. J. Liu, K. Zhou, J. Liu, J. Zhu, Y. Zhen, H. Dong, and W. Hu, Organic-single-crystal vertical field-effect transistors and phototransistors, *Adv. Mater.* 30(44), 1803655 (2018)

106. K. Pei, X. Ren, Z. Zhou, Z. Zhang, X. Ji, and P. K. L. Chan, A high-performance optical memory array based on inhomogeneity of organic semiconductors, *Adv. Mater.* 30(13), 1706647 (2018)

107. X. Wu, Y. Chu, R. Liu, H. E. Katz, and J. Huang, Pursuing polymer dielectric interfacial effect in organic transistors for photosensing performance optimization, *Adv. Sci.* 4(12), 1700442 (2017)